Contribution of Saharan dust to chemical weathering fluxes and associated phosphate release in West Africa

Germain Bayon, Eduardo Garzanti, Pedro Dinis, Daniel Beaufort, Jean-Alix Barrat, Yoan Germain, Anne Trinquier, Marta Barbarano, Brume Overare, Olusegun Adeaga, et al.

Earth Planet. Sci. Lett. 641 (2024) 118845

Contents lists available at ScienceDirect

Earth and Planetary Science Letters

journal homepage: www.elsevier.com/locate/epsl

Contribution of Saharan dust to chemical weathering fluxes and associated phosphate release in West Africa

Germain Bayon [a,*], Eduardo Garzanti [b], Pedro Dinis [c], Daniel Beaufort [d], Jean-Alix Barrat [e,f], Yoan Germain [a], Anne Trinquier [a], Marta Barbarano [b], Brume Overare [g,h], Olusegun Adeaga [i], Nadine Braquet [j]

[a] Univ Brest, CNRS, Ifremer, Geo-Ocean, F-29280 Plouzané, France
[b] Laboratory for Provenance Studies, Department of Earth and Environmental Sciences, University of Milano-Bicocca, 20126 Milano, Italy
[c] Marine and Environmental Sciences Centre (MARE), Aquatic Research Network (ARNET), Department of Earth Sciences, University of Coimbra, 3030-790 Coimbra, Portugal
[d] Université de Poitiers, IC2MP - UMR 7285 - CNRS, F-86073 Poitiers, France
[e] Univ Brest, CNRS, Ifremer, IRD, LEMAR, Institut Universitaire Européen de la Mer (IUEM), F-29280 Plouzané, France
[f] Institut Universitaire de France, Paris, France
[g] Department of Earth Sciences, Memorial University of Newfoundland, St. John's, NL A1B 3 × 5, Canada
[h] Department of Earth Sciences, Federal University of Petroleum Resources, P.M.B 1221, Effurun, Delta State, Nigeria
[i] Department of Geography, University of Lagos, Akoka-Yaba, Lagos, Nigeria
[j] Institut de Recherche pour le Développement IRD – UMR G-eau INRAE, Cedex 5 F-34196, Montpellier, France

ARTICLE INFO

Keywords:
Neodymium
Hafnium
Phosphate minerals
Kaolinite
Bodélé depression
Niger River

ABSTRACT

Huge amounts of mineral dust are produced in northern Africa, representing the largest source of aerosols worldwide. Transatlantic dust transport is known to fertilize soils as far as in the Amazon Basin. Yet, the influence of Saharan dust on chemical weathering fluxes and associated nutrient release in West Africa remains largely overlooked. To address this issue, we analysed clay fractions (<2 μm) of river sediments (n = 37) from across the Niger River basin - the largest river system in West Africa - using neodymium and hafnium isotope compositions as proxies for provenance (ε_{Nd}) and chemical weathering ($\Delta\varepsilon_{Hf\ CLAY}$).

Compared to previously published data for corresponding sand fractions, measured ε_{Nd} values indicate significant size-dependent decoupling for Nd isotopes in most samples, with ε_{Nd} differences between clay and sand fractions yielding values as great as ~26 ε-units. Using mixing models, we show that this discrepancy reflects the overwhelming presence in the studied clay fractions of Harmattan dust blown from the Bodélé Depression in Chad, which we estimate to account for about 40 % of the fine-grained sediment load exported to the Gulf of Guinea. Additionally, significant $\Delta\varepsilon_{Hf\ CLAY}$ variability occurs across the Niger catchment, partly explained by the presence of zircon in clay-size fractions, but also by preferential alteration of dust-borne accessory phosphate minerals in the subtropical regions of the watershed.

Based on these results, we propose that Saharan dust plays a major role in controlling regional patterns of chemical weathering in West Africa, suggesting that enhanced wet deposition of mineral dust in shield areas dominated by transport-limited weathering regime can result in a large increase in weatherability and associated release of phosphorus. These findings have general implications for the importance of mineral aerosols in controlling sediment yield and the supply of weathering-derived nutrients to continental areas bordering large subtropical deserts worldwide.

1. Introduction

The Sahara Desert accounts for about 60 % of annual dust emissions on Earth (Goudie and Middleton, 2001; Laurent et al., 2008). A substantial fraction of atmospheric dust exported from the Sahara comes from the West African El Djouf and the Bodélé Depression (e.g., Koren

* Corresponding author.
E-mail address: gbayon@ifremer.fr (G. Bayon).

https://doi.org/10.1016/j.epsl.2024.118845
Received 7 February 2024; Received in revised form 5 June 2024; Accepted 10 June 2024
Available online 14 June 2024

et al., 2006; Yu et al., 2020; Barkley et al., 2022; Fig. 1), which corresponds to the remnants of ancient Lake Mega-Chad, once the largest lake in Africa, until it dried out a few thousand years ago at the end of the African Humid Period (Armitage et al., 2015). Mineral dust eroded from the Bodélé Depression and/or from other source regions in the Western Sahara are blown over thousands of kilometres by northeasterly and easterly trade winds, respectively (Kalu, 1979; Prospero et al., 2002; Yu et al., 2020; Barkley et al., 2022). Upon deposition and subsequent partial dissolution, Saharan dust plays a crucial role in delivering key nutrients such as phosphorus (P) and iron (Fe) to Atlantic surface waters (Jickells et al., 2005). Dust-borne nutrient additions from Saharan aerosols have been shown to significantly impact soil productivity on Caribbean Islands (Okin et al., 2004; Pett-Ridge, 2009) and in the Amazon rainforest (Swap et al., 1992; Koren et al., 2006; Bristow et al., 2010). In marked contrast, the influence of wind-blown Saharan dust particles and associated fertilization effect on West African soils remains poorly documented (Wilke et al., 1984). This issue is of utmost importance because poor soil fertility in West Africa places severe constraints on ecosystem productivity, with phosphorus generally acting as the most limiting nutrient in these semi-arid regions (Bationo et al., 1991). Atmospheric sources of P and other nutrients can include substantial contribution of organic material derived from biomass burning, which can be readily available for terrestrial ecosystems (Barkley et al., 2019). In contrast, chemical weathering of the mineral component of aeolian dust releases nutrients over longer timescales, ranging from thousands to millions of years, hence playing an important role on the long-term maintenance of productivity, especially in regions covered by old, deeply weathered, soils such as in West Africa (Okin et al., 2004).

In this study, we investigated a suite of river sediments collected from across the Niger River basin (Fig. 1). The Niger River is the main river in West Africa, flowing over ~4200 km from the Guinea highlands to its delta in southern Nigeria, and representing the third largest river basin in Africa after the Congo and the Nile, with a total drainage area of $\sim 2.1 \times 10^6$ km^2. The sand fraction (>63 μm) separated from Niger river sediment has been recently analysed in a companion paper that aimed at investigating both the geological characteristics of source regions and sediment transport dynamics (Pastore et al., 2023). Here, we focus on the clay fraction (<2 μm) of corresponding sediment samples. Fine-grained sediments deposited in river systems integrate the compositional variability of soils developed in upstream regions, and as such are ideal to investigate sediment provenance and chemical weathering at sub-catchment scale. Additionally, the northeasterly Harmattan wind mostly delivers fine mineral dust to West Africa, the so-called Harmattan haze, with median particle size typically ranging from ~0.5 to 10 μm (McTainsh and Walker, 1982; Afeti and Resh, 2000; Utah et al., 2005). Separated clay fractions hence appear well suited for tracing dust inputs to surface sediments in West Africa.

The approach used in this study combines the application of neodymium (Nd) and hafnium (Hf) isotopes, in addition to clay mineralogy, and major- and trace-element abundances. Radiogenic isotopes are powerful proxies for sediment provenance and the tracing of Saharan mineral dust (Grousset et al., 1998; Abouchami et al., 2013; Bozlaker et al., 2018; Jewell et al., 2021; Guinoiseau et al., 2022). The main source regions of mineral dust in North Africa are relatively well characterized for neodymium (Nd), strontium (Sr), and lead (Pb) isotopes, albeit showing overlap and significant intra-compositional variability (Abouchami et al., 2013; Jewell et al., 2021; Guinoiseau et al., 2022). Unlike Sr isotopes, surface sediments and atmospheric particulates from a given source area generally display limited grain-size variability for Nd isotopes, which makes them particularly well-suited for provenance investigations (e.g., Meyer et al., 2011; Bayon et al., 2015). In marked contrast, Hf isotopes are strongly decoupled during sediment transport and continental chemical weathering (Patchett et al., 1984; Bayon et al., 2006; Dausmann et al., 2019). Preferential dissolution of phosphate-bearing minerals releases a fraction of very radiogenic Hf (with high ε_{Hf} values) to surface environments, which can be

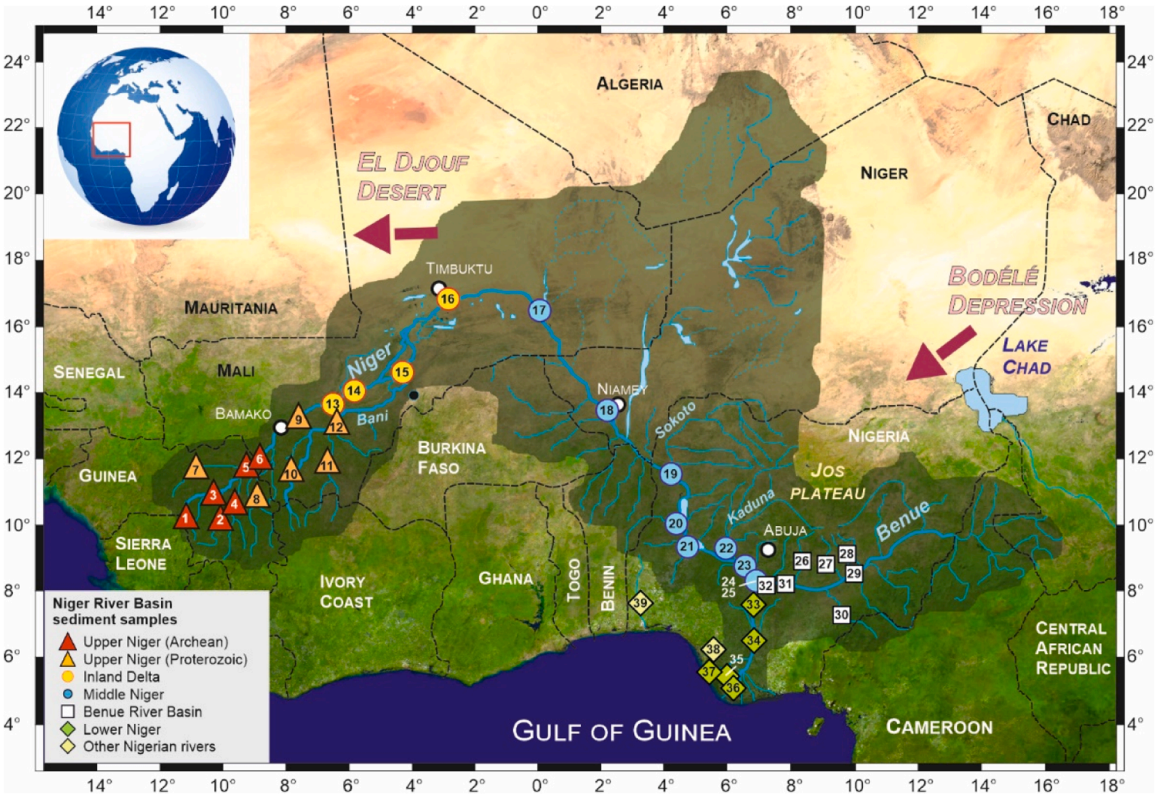

Fig. 1. The Niger River Basin and location of studied river sediment samples in West Africa. The red arrows correspond to the main trajectories of Saharan dust transport from the Bodélé Depression (Harmattan wind) and El Djouf Desert, i.e. the two main source regions of mineral dust in North Africa (Prospero et al., 2002).

subsequently incorporated into clay-mineral phases formed in soils (Bayon et al., 2016). In a ε_{Nd} vs ε_{Hf} diagram, clay fractions of aeolian dust and river sediments worldwide define a distinctive correlation referred to as the Clay Array (Zhao et al., 2014; Bayon et al., 2016). The vertical deviation of Hf isotopes relative to the Clay Array (termed $\Delta\varepsilon_{Hf\ CLAY}$) provides a robust proxy for chemical weathering (Bayon et al., 2016, 2022; Chen et al., 2023), which, unlike conventional weathering indices, uniquely relates to the degree of alteration of phosphate minerals. Therefore, the combination of Nd and Hf isotopes in clay fractions is ideally suited for tracing dust inputs and associated phosphorus release in West African soils.

2. Climate setting and geology of the Niger catchment

The Upper Niger river is sourced from the Guinea highlands, one of the wettest regions in West Africa, before flowing northeastward across a vast alluvial floodplain located in central Mali - the Inland Delta (Fig. 1), where most of the Upper Niger water discharge is lost due to seepage and evaporation (Mahé et al., 2009). Upon reaching the southern fringes of the Sahara Desert, the Middle Niger forms a great bend before flowing southeastward until it meets the Benue River, its largest tributary sourced from the Adamawa Plateau in northern Cameroon. Finally, after the confluence with the Benue, the Lower Niger flows southward forming a large delta and discharging into the Atlantic Ocean (Fig. 1). Along its course, the Niger River crosses several climatic zones, from wet tropical climate (GuineoCongolian) in headwater areas (mean annual precipitation >2.2 m) to semi-arid (Sahelian; 0.15–0.6 m) and arid climate (Saharan; <0.15 m) to the north of the Inland Delta. After the wide bend across the Sahel, the Niger River flows across regions experiencing wetter climate. While rainfall in West Africa mostly occurs during the summer season, following northward migration of the intertropical convergence zone, the Harmattan generally blows during winter months (Kalu, 1979), delivering substantial amounts of Saharan mineral dust to West Africa, most from the Bodélé Depression (Fig. 1). Wet dust deposition also contributes significantly to annual dust deposition rates in West Africa, associated with precipitation and cloud scavenging (e.g., Schepanski et al., 2009; Marticorena et al., 2017; Schepanski, 2018).

In Niger headwaters, sediment load is derived from the Archean Man Shield (Thiéblemont et al., 2004). Downstream, the Upper Niger flows across Paleoproterozoic and Neoproterozoic-Cambrian sedimentary formations of the Siguiri (Lebrun et al., 2016) and Taoudeni basins (Deynoux et al., 2006), respectively. The Baoulé and Bagoé headwater branches of the Bani River mostly drain Paleoproterozoic plutonic and metamorphic rocks of the Baoulé-Mossi domain (Parra-Avila et al., 2016). Downstream of the Inland Delta, the Sahelian Niger carries mostly sand recycled from Saharan dunes (Pastore et al., 2023). The sediment flux is progressively restored in Nigeria, largely by the Sokoto and Kaduna rivers (Fig. 1), which drain the northern Nigerian basement complex composed of Mesoarchean to Paleoproterozoic gneisses and schists. Finally, the Benue River, which originates from the Adamawa volcanic highlands and flows along the Benue Through - a failed rift filled with thick Cretaceous sediments overlying crystalline basement rocks - receives sediment from tributaries originating from the Jos Plateau (Fig. 1), where Jurassic granites and Cenozoic basalts are exposed (Ofoegbu, 1985).

3. Materials and methods

A total of 37 riverbank sediment samples were collected from across the Niger River basin mostly between 2020 and 2022 (Fig. 1). Twelve samples were collected from the Upper Niger headwater catchment and tributaries in Guinea and Mali, 4 in the Inland Delta area in central Mali, 8 downstream of Gao (Mali) and Niamey (Niger) along the Middle Niger, 7 from the Benue River and tributaries, and 5 from the Lower Niger. Two additional samples were recovered from coastal rivers in southern Nigeria. Full information on sampling sites is provided in Supplementary Table S1.

Prior to geochemical analyses, clay (<2 μm) fractions of river sediment samples were separated by low-speed centrifugation, following removal of carbonates, Fe-oxide phases and organic matter by sequential leaching (Bayon et al., 2015). Between ~20 and 50 mg of powdered samples were digested using HF-HNO_3—HCl at 140 °C for 5 days. Major and trace element abundances were determined at the Pôle Spectrométrie Océan (Brest) with a Thermo Scientific Element XR sector field ICP-MS, using the Tm addition method and after correction from isobaric interferences (Barrat et al. 1996). The precision for major and trace elements was better than 3 %. The accuracy of measured concentrations (typically <5 %) was assessed by analysing three certified reference materials (BCR-2, W-2, JBC-1).

Hafnium and neodymium were purified by ion exchange chromatography (Bayon et al., 2016), and Hf-Nd isotope measurements were conducted at the Pôle Spectrométrie Océan (Brest) using a Thermo Scientific Neptune multi-collector ICP-MS. Hf and Nd isotopic compositions were determined using sample-standard bracketing, by analysing AMES and Nd Spex standard solutions every two samples, respectively. All measured Hf and Nd isotopic ratios were corrected from mass bias using $^{179}Hf/^{177}Hf = 0.7325$ and $^{146}Nd/^{144}Nd = 0.7129$, respectively. Hf and Nd isotopic ratios are expressed using the epsilon notation, with $\varepsilon_{Hf} = [(^{176}Hf/^{177}Hf)_{sample} / (^{176}Hf/^{177}Hf)_{CHUR} - 1] \times 10{,}000$ and $\varepsilon_{Nd} = [(^{143}Nd/^{144}Nd)_{sample} / (^{143}Nd/^{144}Nd)_{CHUR} - 1] \times 10{,}000$; using Chondritic Uniform Reservoir (CHUR) values of 0.282785 and 0.512630 for Hf and Nd isotopic ratios, respectively (Bouvier et al., 2008). During analytical sessions, Hf and Nd isotopic compositions of JMC-475 and JNdi-1 solutions yielded 0.282161 ± 0.000007 (2 SD; $n = 10$) and 0.512114 ± 0.000011 (2 SD; $n = 8$) values similar to reference values, which correspond to an external reproducibility of 0.23 and 0.22 ε-units, respectively.

A total of 17 samples were analysed for clay mineralogy on <2 μm fractions by X-ray diffraction (XRD) using a PANalytical Aeris instrument equipped with a Cu tube. Operational conditions were 15 kV and 40 mA. XRD analyses were performed on air dried slides (2–30° 2θ) and after solvation with ethylene-glycol and heating at 550 °C (2–15° 2θ). Mineral proportions were evaluated semi-quantitatively based on the areas of characteristic reflections identified in the diffractograms.

Finally, two samples of separated clay fractions from the Upper Niger (#4) and the Benue River (#32) were selected for detailed examination using a scanning electron microscope (JEOL JSM IT500; Univ. Poitiers) equipped with secondary electron (SE) and backscatter electron (BSE) detectors, and coupled with a Bruker Linxeye energy dispersive X-ray spectrometer (EDS). Before analysis, samples were mounted on glass slides using epoxy resin, diamond polished and coated with carbon. Specific areas containing accessory mineral phases were selected for high-resolution BSE imaging (15 nm pixel resolution) and chemical mapping by EDS.

4. Results

4.1. Clay mineralogy, major and trace element data

Clay mineralogy, major and trace element abundances are provided in Supplementary Table S1. Both clay-mineral and major-element abundances in the studied clay fractions display longitudinal trends across the Niger River basin (Fig. 2). Kaolinite is the dominant clay mineral in all samples, particularly in the Upper Niger catchment, where almost pure kaolinite (up to 100 %) indicates extensive contribution from intensively weathered ferralitic soils or laterites. While kaolinite content decreases eastward to ~60 % (Fig. 2A), illite correspondingly increases progressively from ~0 to 40 % (Fig. 2B). Both kaolinite and illite co-vary with Al_2O_3 and K_2O abundances, respectively (Fig. 2A,B). Apart from one sample from the Middle Niger (#25; with smectite ~18 %), all studied samples display negligible smectite contents (<5 %).

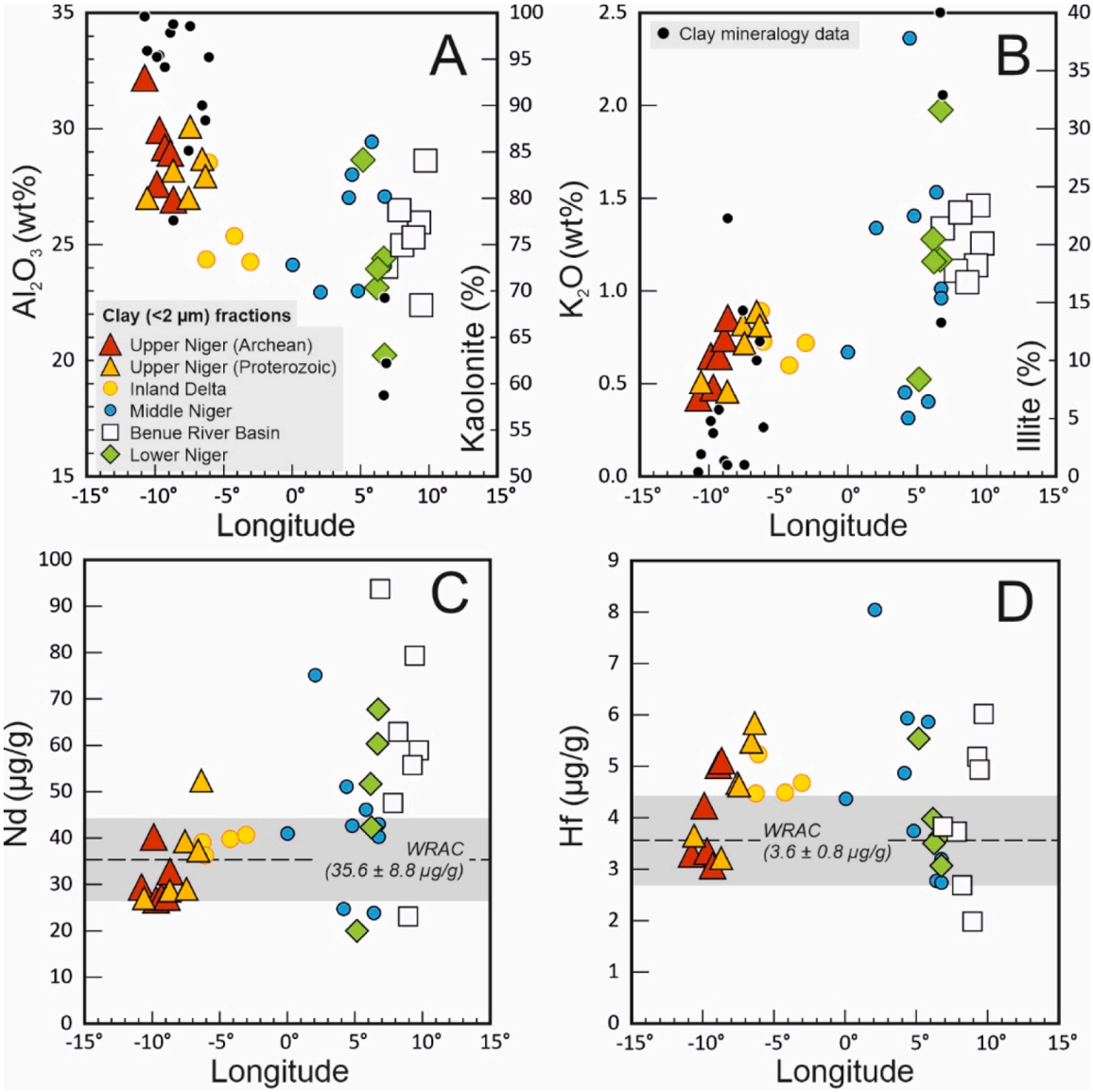

Fig. 2. Longitudinal distribution patterns of selected clay mineral, major and trace element abundances in the clay-size fraction of studied river sediments. (A) Al_2O_3 (wt %) and kaolinite (%). (B) K_2O (wt %) and illite (%). (C) Nd (µg/g). (D) Hf (µg/g). The horizontal grey bands refer to the average Nd and Hf abundances in the clay-size fraction of river sediments from large river systems worldwide or WRAC (World Average River Clay; Bayon et al., 2015).

Note that the chemical index of alteration (CIA) varies from ~90 to 100 in the studied clay fractions (Table S1), exhibiting a strong negative correlation with K_2O ($R^2 = 0.89$; plot not shown here). As for illite and K_2O, Nd content progressively increases from west-to-east in the clay fraction, from ~26 ppm in the Upper Niger headwater catchment up to 93 ppm in the Benue River basin, where Nd abundance levels vary significantly (Fig. 2C). Such high Nd abundances clearly depart from the common range of Nd concentrations in clays from large river systems worldwide (35.6 ± 8.8 ppm; Fig. 2C; Bayon et al., 2015). Similarly, anomalously high levels of Hf in the studied samples (up to 8.1 ppm) relative to other river clays worldwide (3.6 ± 0.8 ppm; Fig. 2D; Bayon et al., 2015) point towards the presence of minute zircon grains in the studied samples. Finally, shale-normalized REE abundances for clay fractions display similar patterns across the entire Niger watershed (Supplementary Figure S1), generally indicating gradual enrichment from the heavy- to the light- REE.

4.2. Nd and Hf isotopes

The Nd and Hf isotope data are reported in Table 1. The Nd isotope composition of clay fractions progressively increases from the uppermost Niger catchment region where Archean basement rocks are exposed, with ε_{Nd} values varying from −29.0 to −17.8, to the Benue River and Lower Niger watersheds (Fig. 3A), where all but one of the studied samples display similar ε_{Nd} composition ($\varepsilon_{Nd} = -11.8 \pm 0.5$; 1 SD; $n = 11$). The evidence that river clays from the Benue River and Lower Niger share similar Nd isotope signatures is consistent with recent findings suggesting a major sediment contribution from the Benue River to the sediment load exported by the Niger River to the Gulf of Guinea (Pastore et al., 2023). In the Upper Niger watershed, measured ε_{Nd} data for clay fractions are significantly more radiogenic than values for corresponding sand fractions (Pastore et al., 2023), with ε_{Nd} differences between the two size fractions ($\Delta\varepsilon_{Nd\ CLAY\text{-}SAND}$) ranging between 2.5 and 26.3 ε-units (Table 1).

Expectedly, the clay fractions from the Niger River basin plot near the correlation trend defined by the Clay Array in the ε_{Nd} vs ε_{Hf} diagram

Table 1
Nd-Hf isotope compositions of clay-size (<2 μm) fractions of river sediments from the Niger River Basin.

#	N	River	Sampling site	Country	Long (°)	$^{143}Nd/^{144}Nd$	2 se	ε_{Nd} CLAY	ε_{Nd} SAND	$\Delta\varepsilon_{Nd\ CLAY-SAND}$ *	$^{176}Hf/^{177}Hf$	2 se	ε_{Hf} CLAY	$\triangle\varepsilon_{Hf\ CLAY}$
1	6250	Upper Niger	Faranah	Guinea	−10.77	0.511144	±10	−29.0	−41.0	12.0	0.282488	±5	−10.5	6.9
2	6252	Niandan	Baro	Guinea	−9.69	0.511283	±8	−26.3	–	–	0.282497	±6	−10.2	5.1
3	6251	Upper Niger	Kouroussa	Guinea	−9.87	0.511487	±6	−22.3	−28.4	6.1	0.282462	±6	−11.4	0.7
4	6253	Milo	Kankan	Guinea	−9.29	0.511367	±9	−24.6	−29.3	4.7	0.282662	±6	−4.3	9.7
5	6255	Upper Niger	Dialakoro	Guinea	−8.90	0.511712	±6	−17.9	−36.2	18.3	0.282512	±6	−9.6	−0.9
6	6256	Upper Niger	Banankoro	Mali	−8.66	0.511716	±6	−17.8	−44.1	26.3	0.282416	±5	−13.0	−4.4
7	6254	Tinkisso	Tinkisso	Guinea	−10.58	0.511601	±8	−20.1	−29.7	9.6	0.282585	±6	−7.1	3.4
8	6257	Sankarani	Mandiana	Guinea	−8.68	0.511546	±9	−21.1	−29.4	8.2	0.282711	±6	−2.6	8.7
9	6258	Upper Niger	Koulikoro	Mali	−7.55	0.511642	±9	−19.3	−23.4	4.1	0.282466	±9	−11.3	−1.5
10	6261	Bagoé	Bada	Mali	−6.57	0.511793	±9	−16.3	−18.8	2.5	0.282487	±4	−10.5	−3.0
11	6262	Baoulé	Bougouni	Mali	−7.44	0.511846	±21	−15.3	−19.9	4.7	0.282556	±6	−8.1	−1.4
12	6263	Bani	Kana	Mali	−6.34	0.511904	±6	−14.2	−18.5	4.4	0.282590	±5	−6.9	−1.1
13	6259	Inner Delta	Ségou	Mali	−6.26	0.511724	±11	−17.7	−21.8	4.2	–		–	–
14	6260	Inner Delta	Markala	Mali	−6.07	0.511710	±7	−17.9	−31.2	13.3	0.282540	±6	−8.7	0.1
15	6264	Inner Delta	Mopti	Mali	−4.20	0.511673	±7	−18.7	−23.2	4.5	0.282558	±5	−8.0	1.3
16	6265	Inner Delta	Timbuktú	Mali	−3.02	0.511774	±6	−16.7	−15.0	−1.7	–		–	–
17	6266	Sahelian Niger	Gao	Mali	0.05	0.511890	±7	−14.4	–	–	0.282608	±5	−6.3	−0.2
18	6231	Sahelian Niger	Niamey	Niger	2.10	0.511809	±6	−16.0	−10.5	−5.6	0.282492	±4	−10.4	−3.1
19	6075	Sokoto	Tunga Baushe	Nigeria	4.17	0.512002	±11	−12.2	–	–	–		–	–
20	6078	Oli	Lesu	Nigeria	4.39	0.511797	±7	−16.2	−18.2	1.9	0.282562	±6	−7.9	−0.4
21	6079	Middle Niger	Jebba	Nigeria	4.82	0.511757	±8	−17.0	−22.5	5.5	–		–	–
22	6080	Kaduna	Wuya	Nigeria	5.84	0.511812	±6	−16.0	−21.3	5.3	0.282554	±6	−8.2	−1.0
23	6081	Middle Niger	Baro	Nigeria	6.42	0.512221	±7	−8.0	−8.0	0.0	0.282766	±8	−0.7	0.3
24	6082	Middle Niger	Adaha	Nigeria	6.77	0.511891	±8	−14.4	−19.8	5.4	0.282646	±7	−4.9	1.1
25	6232	Middle Niger	Jamata	Nigeria	6.77	0.511686	±6	−18.4	−16.4	−2.0	0.282648	±8	−4.8	4.3
26	6084	Mada	Lafia	Nigeria	8.22	0.512043	±6	−11.4	−10.2	−1.2	0.282762	±7	−0.8	2.9
27	6085	Dep	Namu	Nigeria	8.95	0.512235	±11	−7.7	−10.2	2.5	–		–	–
28	6086	Shemanker	Peshiep	Nigeria	9.44	0.511970	±5	−12.9	−16.0	3.1	0.282626	±6	−5.6	−0.8
29	6087	Benue	Ibi	Nigeria	9.74	0.512014	±10	−12.0	−12.7	0.7	–		–	–
30	6088	Katsina Ala	Katsina Ala	Nigeria	9.28	0.512022	±6	−11.9	−13.9	2.1	–		–	–
31	6090	Benue	Shata	Nigeria	7.84	0.512019	±10	−11.9	−11.5	−0.4	–		–	–
32	6233	Benue	Mozum	Nigeria	6.89	0.512038	±7	−11.6	−14.1	2.6	0.282783	±6	−0.1	3.7
33	6234	Lower Niger	Itobe	Nigeria	6.70	0.512032	±6	−11.7	−17.1	5.4	0.282790	±6	0.2	4.0
34	6092	Lower Niger	Asaba	Nigeria	6.75	0.512009	±7	−12.1	−11.6	−0.5	–		–	–
35	6103	Lower Niger	Patani	Nigeria	6.19	0.512015	±7	−12.0	−14.3	2.3	0.282698	±6	−3.1	1.0
36	6104	Nun	Yenagoa	Nigeria	6.25	0.512046	±5	−11.4	−18.4	7.1	–		–	–
37	6097	Niger Delta	Ugborodo	Nigeria	5.18	0.512057	±14	−11.2	−12.2	1.0	0.282628	±8	−5.6	−2.1
38	6101	Benin	Koko	Nigeria	5.46	0.512031	±23	−11.7	−14.3	2.7	–		–	–
39	6100	Ogun	Abeokuta	Nigeria	3.32	0.511743	±7	−17.3	−18.5	1.2	–		–	–

* Nd isotope data for Niger sand fractions are from Pastore et al. (2023).

(Fig. 3B). The vertical deviation of measured Hf isotopic compositions relative to the Clay Array displays significant variability with $\triangle\varepsilon_{Hf\ CLAY}$ values varying between −4.4 and +9.6 (Table 1), hence almost encompassing the observed range of values for river clays worldwide (from −11.3 to +15.5; Bayon et al., 2016, 2022). In marked contrast, corresponding sand fractions (Pastore et al., 2023) plot below the Terrestrial Array defined by all igneous rocks and bulk sedimentary rocks (Fig. 3B; Vervoort et al., 2011), reflecting the overwhelming presence of zircon, a highly resistant Hf-bearing accessory mineral which typically dominates the Hf budget in silt and sand and is generally associated with unradiogenic (low) ε_{Hf} signatures (Patchett et al., 1984; Bayon et al., 2009, 2016).

4.3. SEM observations

The separated clay fractions investigated by SEM-EDS display abundant micro-grains of iron oxides (hematite), titanium oxides (rutile, anatase) and mixed Fe-Ti oxides (ilmenite, Ti-magnetite) (Fig. 4). Both samples also host discrete sub-μm grains of zircon, quartz and white mica. For the Upper Niger clay fraction (sample #4), our observations provide direct evidence for the presence of large amounts of light-REE (i.e. La, Ce, Nd) in minute minerals with a chemical composition indicative of LREE-rich aluminium-phosphate-sulfate (APS) minerals dominated by the florencite end-member [$LREEAl_3(PO_4)_2(OH)_6$] (Fig. 4A). The Benue River clay fraction (sample #32) contains grains of LREE- and Th-bearing monazite (Fig. 4B), together with Mn-bearing titanium-iron oxides (ilmenite).

5. Discussion

5.1. Contribution of Saharan mineral dust to the clay fraction of Niger River sediments

A striking feature of our results is the evidence for different Nd isotopic signatures in clay-sand pairs. This effect is particularly pronounced in the Upper Niger catchment, where $\Delta\varepsilon_{Nd\ CLAY-SAND}$ reaches values up to ~26 ε-units. Chemical weathering is unlikely to decouple Nd isotopes significantly on continents. Although incongruent silicate weathering in soils overlying Precambrian crystalline rocks can result in preferential dissolution of minerals with slightly different Nd isotopic compositions, the corresponding ε_{Nd} decoupling among different soil horizons generally remains limited to a few ε-units (Ohlander et al., 2000). Similarly, a comparison of Nd isotopes in both clay and silt fractions of river sediments worldwide indicates a limited size-dependent Nd isotope decoupling in catchments draining Precambrian crystalline rocks, with a mean $\Delta\varepsilon_{Nd\ CLAY-SILT}$ value of −0.2 ± 1.4 (1SD; n = 11; Bayon et al., 2015). Therefore, the observed size-dependent ε_{Nd} discrepancy is best explained as reflecting markedly differing provenance between clay and

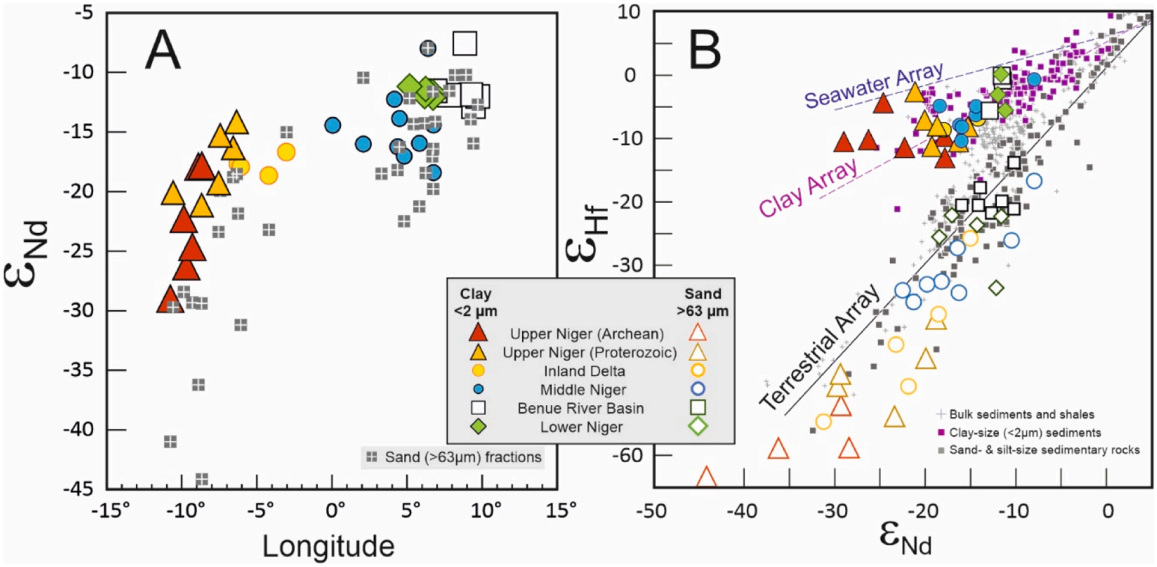

Fig. 3. Neodymium (ε_{Nd}) and hafnium (ε_{Hf}) isotopic compositions of the clay (<2 μm) fraction of river sediments from the Niger River Basin. (A) Longitudinal distribution pattern of ε_{Nd} in river clays across the Niger catchment. White crosses refer to ε_{Nd} values for corresponding sand (>63 μm) fractions (Pastore et al., 2023). (B) ε_{Nd} vs ε_{Hf} diagram. The Clay Array ($\varepsilon_{Hf} = 0.78 \times \varepsilon_{Nd} + 5.23$) refers to the linear regression based on fluvial clays and clay fractions of modern sediments (Bayon et al., 2016; and references therein). The Terrestrial Array corresponds to the correlation defined by all terrestrial rocks, including bulk sediments and shales (Vervoort et al., 1999, 2011). Hf-Nd isotope data for corresponding sand fractions in the Niger River Basin (Pastore et al., 2023) are shown for comparison together with literature data for other detrital sand fractions, river silts and sandstones (Vervoort et al., 1999, 2011; Garçon et al., 2013; Bayon et al., 2016). The Seawater Array include Nd-Hf isotope data for seawater and marine ferromanganese crusts and nodules (Albarède et al., 1998).

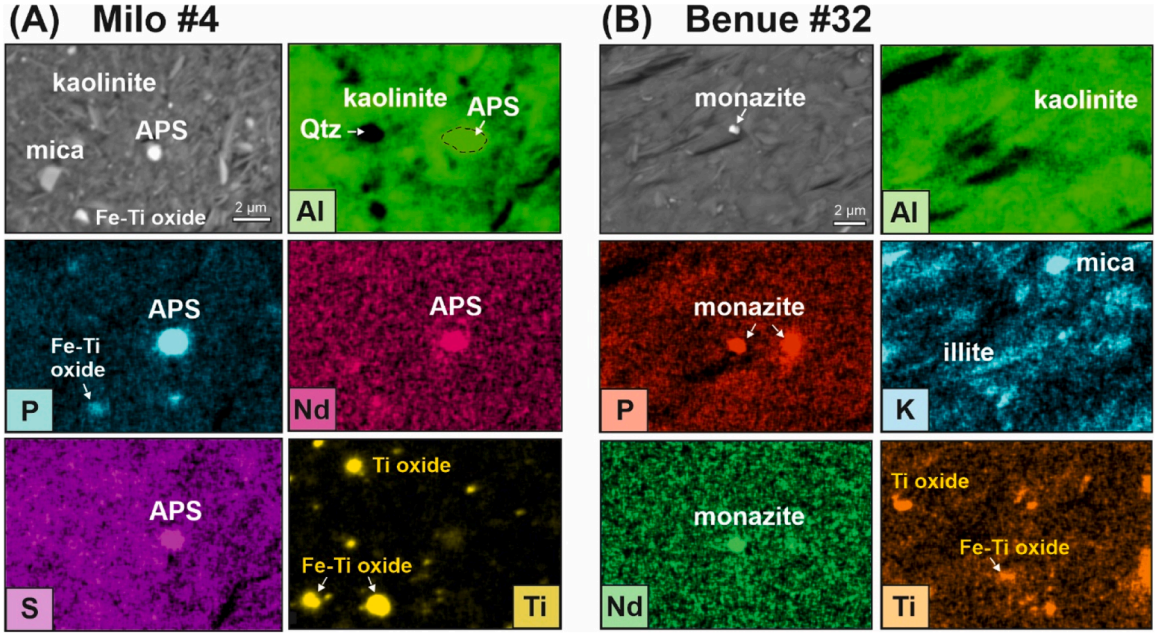

Fig. 4. SEM-EDS observations and elemental mapping of clay fractions from the Niger River basin. (A) Sample #4 (Milo River; Upper Niger basin). The SEM-BSE image (grey) shows the presence of florencite, a LREE-secondary aluminium-phosphate-sulfate (APS) mineral of the crandallite series, which typically forms in tropical soils following alteration of primary phosphate minerals (e.g., apatite, monazite). (B) Sample #32 (Benue River; Upper Niger basin). The SEM-BSE image (grey) indicates the presence of Th- and LREE-bearing monazite, most likely associated with the deposition of Harmattan dust from the Bodélé Depression. Both samples also show evidence for numerous grains of iron oxides, titanium oxides, and mixed Ti-Fe oxides.

sand fractions, indicating in turn a substantial contribution of <2 μm mineral dust blown from the nearby Sahara Desert. To test this hypothesis, we consider a ε_{Nd} vs Sm/Nd diagram, in which co-genetic rocks and resulting erosional products should align along pseudo-isochron slopes (Fig. 5). In the uppermost Archean catchment of the Upper Niger, all river sand samples but one plot within the field defined by Archean gneisses from the Man shield (Kouamelan et al., 1997). Similarly, sand fractions collected from the Upper Niger catchment and tributaries draining mainly Paleoproterozoic rocks mostly fall within the field defined by metamorphic rocks of the corresponding Baoulé-Mossi domain (Boher et al., 1992). These observations clearly suggest that river sands in the Upper Niger catchment are derived from erosion of local bedrock units. In marked contrast, corresponding clay fractions generally depart significantly from these pseudo-isochron trends,

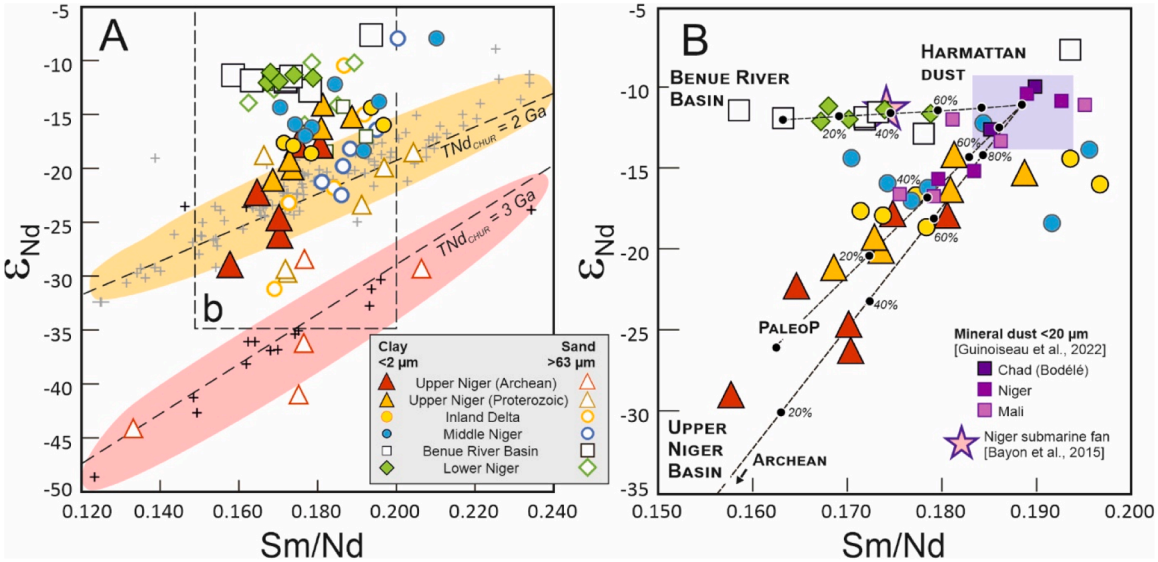

Fig. 5. Nd isotope constraints on sediment provenance. (A) Plot of ε_{Nd} vs Sm/Nd ratios for clay (this study) and sand fractions (Pastore et al., 2023) of river sediments from the Niger catchment. Also shown for comparison are Nd isotope and Sm/Nd data for Archean gneisses from the Man shield (black crosses; Kouamelan et al., 1997) and Paleoproterozoic metamorphic rocks from the Baoulé-Mossi domain (grey crosses; Boher et al., 1992), which define pseudo-isochron relationships visualized by pink and yellow fields, respectively. Dashed lines indicate theoretical ε_{Nd} vs Sm/Nd relationships for rocks displaying CHUR Nd model ages of 3 Ga and 2 Ga, calculated using $^{147}Sm/^{144}Nd = Sm/Nd \times 0.6049$, the decay constant of ^{147}Sm ($\lambda = 6.54 \times 10^{-12}$), and present-day $^{143}Nd/^{144}Nd$ and $^{147}Sm/^{144}Nd$ CHUR values of 0.512630 and 0.1960, respectively (Bouvier et al., 2008). (B) Close-up into the ε_{Nd} vs Sm/Nd relationship for clay fractions of Niger River sediments and for <20 µm mineral dust samples from Tchad (Bodélé Depression), Niger and central Mali (Guinoiseau et al., 2022). Inferred end-member compositions of <2 µm detritus from the Upper Niger Archean basement ($\varepsilon_{Nd} = -40$; Sm/Nd = 0.150; Kouamelan et al., 1997), Upper Niger Paleoproterozoic basement (−26; 0.163; Boher et al., 1992), Benue River Basin (−11.9; 0.163; this study) and Harmattan dust (−11.0; 0.188; Guinoiseau et al., 2022) are shown for comparison. Mixing lines between the different end-members are shown; small black circles correspond to 20 %, 40 %, 60 % and 80 % relative contributions.

suggesting the presence of additional components (Fig. 5A). In Fig. 5B, river clays from the Upper Niger catchment are well aligned along mixing lines between 'local' end-members for both Archean and Paleoproterozoic basements, and a field defined by mineral dust samples from Chad, Niger and Mali (Guinoiseau et al., 2022). This observation clearly indicates that aeolian particles blown from the Bodélé Depression and/or Western Saharan dust source areas can contribute significantly to the clay fraction in the Upper Niger catchment (Fig. 5B). Interestingly, river clays from both the Benue and Lower Niger basins are also aligned along a distinctive mixing trend that suggests strong influence of Harmattan dust from the Bodélé Depression (Fig. 5B). The observed relationship seems to exclude significant dust contribution from Western Saharan source areas (e.g., Mali, Southern Algeria, Central Niger), which carry distinctive unradiogenic ε_{Nd} signatures ranging from ~ −17 to −13 (Jewell et al., 2021; Guinoiseau et al., 2022). Surface sediments in the Bodélé Depression display significant compositional variability for Nd isotopes, which reflects mixing between geochemically-distinct source areas (Abouchami et al., 2013; Jewell et al., 2021), with inferred average ε_{Nd} compositions ranging from −11.8 ± 1.8 (Guinoiseau et al., 2022) to −10.0 ± 3.9 (Jewell et al., 2021). Considering representative ε_{Nd} and Sm/Nd values for Harmattan dust (Guinoiseau et al., 2022) and a putative end-member for 'pure' Benue River material (i.e. derived from local catchment-scale bedrock weathering) inferred from sample #31 collected ~120 km upstream of the Niger-Benue confluence (Fig. 1), we tentatively estimate, based on our data, that the <2 µm sediment load carried by the Lower Niger includes between ~20 % to 60 % of Saharan dust (Fig. 5B). This result is corroborated by data for both terrigenous clay and silt in marine sediment from the Niger Delta margin (Bayon et al., 2015), which confirm that Saharan dust may account for ~40 % of the finest sediment fraction exported by the Niger River to the Atlantic Ocean (Fig. 5B).

5.2. *Longitudinal geochemical gradients explained by settling of Saharan dust particles*

The degree of Hf-Nd isotope decoupling in the clay fraction of river sediments worldwide exhibits strong relationships with mean annual temperature and precipitation levels in corresponding basins, as well as with indices of chemical weathering (Bayon et al., 2016, 2022). This finding has paved the way for the application of $\Delta\varepsilon_{Hf\ CLAY}$ as a proxy for continental weathering in the sedimentary record, with positive values being generally interpreted as indicative of periods of relatively intense chemical weathering associated with enhanced alteration of radiogenic phosphate minerals (Bayon et al., 2022; Chen et al., 2023). In this study, many clay fractions display highly radiogenic Hf isotope compositions, thereby suggesting that the observed Nd-Hf isotope variability across the Niger catchment could link to various degrees of chemical weathering. However, an important prerequisite for using Hf-Nd isotopes as a weathering proxy is that measured $\Delta\varepsilon_{Hf\ CLAY}$ values are not controlled by the presence of unradiogenic zircon. In this study, the strong relationship observed between $\Delta\varepsilon_{Hf\ CLAY}$ and Zr abundances clearly point to the presence of dust-borne zircon grains in studied clay samples and to its influence on measured ε_{Hf} values (Fig. 6A). Preferential depletion of dense zircon minerals during transatlantic dust transport has already been reported in previous Nd-Hf isotope investigations of Saharan dust, showing how such 'zircon effect' could modify the ε_{Hf} composition of wind-blown particles with increasing transport distance from dust source regions (Rickli et al., 2010; Aarons et al., 2013; Pourmand et al., 2014; van der Does et al., 2018; Zhao et al., 2018). The presence of small grains of zircon in studied clay fractions is also supported by our SEM-EDS observations.

Dry deposition of dust particles is largely controlled by gravitational settling (Schepanski et al., 2009); a process that explains why dust particle size rapidly decreases downwind of the Bodélé Depression (Utah et al., 2005), from a mean diameter of ~9 µm in northern Nigeria (McTainsh and Walker, 1982) to ~1 µm in southern Ghana (Afeti and

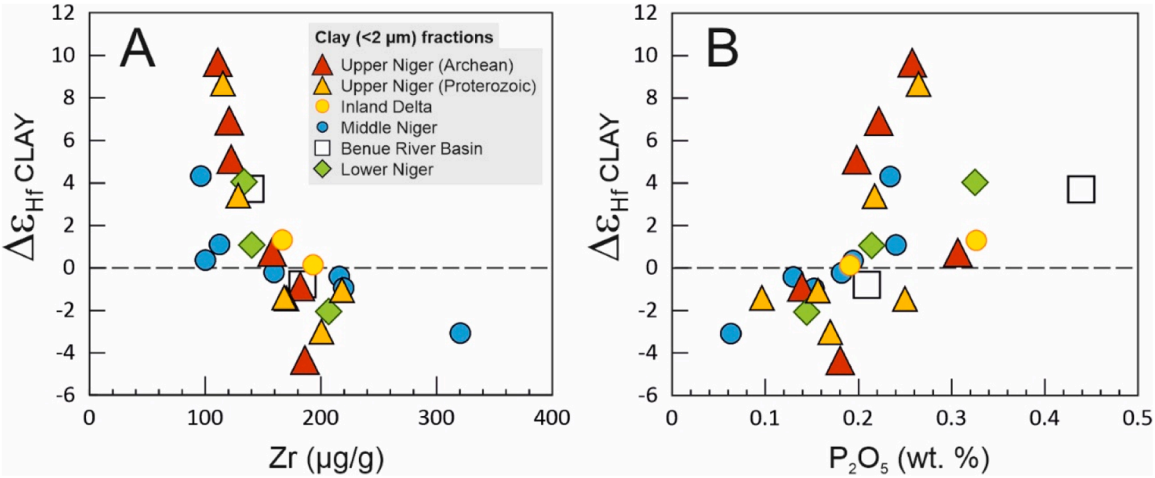

Fig. 6. Influence of zircon and phosphate-bearing minerals on the degree of Nd-Hf isotope decoupling ($\Delta\varepsilon_{Hf\ CLAY}$) in Niger River sediments. (A) Relationship between $\Delta\varepsilon_{Hf\ CLAY}$ and Zr abundances, illustrating the 'zircon effect' in studied clay fractions. (B) Relationship between $\Delta\varepsilon_{Hf\ CLAY}$ and P_2O_5 abundances, interpreted as reflecting the presence of wind-blown monazite, apatite and/or secondary phosphate minerals (e.g., rhabdophane, florencite) formed in kaolinite-bearing subtropical soils during chemical weathering.

Resh, 2000). Gravitational settling during Harmattan dust transport may partly account for the observed westward depletion in illite and K abundances in this study (Fig. 2), consistently with decreasing input of illite-bearing mineral dust from the Bodélé Depression along its south-westerly trajectory (Wilke et al., 1984). Other elements also display pronounced longitudinal geochemical gradients across the Niger River watershed. This is the case for Nd (Figure 2; coefficient of determination with longitude $R^2 = 0.26$), but also for other REE, especially Ce ($R^2 = 0.31$), U ($R^2 = 0.42$) and to a lesser extent Th ($R^2 = 0.15$) (plots not shown here), which collectively point towards the possible influence of monazite - an accessory phosphate mineral significantly enriched in light-REE, Th and U - in clay sediments across the Niger watershed. This hypothesis is fully consistent with SEM-EDS observations, which provide direct evidence for the presence of Th- and LREE-bearing monazite in the clay fraction of sample #32 (Benue River; Fig. 4B). Several studies also reported the presence of monazite and other phosphate minerals (apatite) in Harmattan dust deposited in West Africa (e.g., Wilke et al., 1984; Falaiye and Aweda, 2018). Because monazite is a very dense mineral, its preferential settling during Harmattan dust transport most likely accounts for the observed longitudinal trends for Nd, Ce, Th and U across the Niger catchment, and also partly explains some of the observed $\Delta\varepsilon_{Hf\ CLAY}$ variability (Fig. 6B). Interestingly, Hf (and Zr) abundances do not indicate any significant longitudinal gradient across the Niger River basin, displaying instead substantial variability in both eastern and western parts of the watershed (Fig. 2). To a first approximation, this observation suggests that wind-blown clay-size zircon deposited in the Upper Niger catchment may derive from multiple sources, whereas aeolian inputs of phosphate-bearing minerals would be dominantly sourced from the Bodélé Depression. Proximal Western Saharan dust source regions such as the El Djouf Desert in Mali (Fig. 1), an important regional contributor of dust from North Africa (e.g., Prospero et al., 2002), may represent a plausible additional source for <2 µm zircons in the Upper Niger catchment. This hypothesis is consistent with the fact that a few dust samples from central Mali (Guinoiseau et al., 2022) plot well in the field defined by corresponding clay fractions in the ε_{Nd} vs Sm/Nd diagram (Fig. 5B).

To summarize, our data suggest that the transport of illite-bearing dust associated with Harmattan winds is accompanied by preferential deposition of zircon and monazite in West African surface sediments, influencing elemental and Nd and Hf isotope geochemistry of clay across the Niger River basin.

5.3. *Influence of Saharan dust on chemical weathering and associated P release*

As discussed above, our data suggest that the spatial distribution of Nd and Hf isotopes in clay across the Niger watershed is influenced by Saharan dust deposition and presence of wind-blown accessory minerals. To investigate how the presence of mineral dust in West African soils may affect chemical weathering, we explore below the relationships between climate, dust deposition rates, and $\Delta\varepsilon_{Hf\ CLAY}$ at the catchment scale (Fig. 7). An important feature of our results is that negative $\Delta\varepsilon_{Hf\ CLAY}$ values across the Niger catchment generally occur in the Sudanian-Sahelian region, i.e. in the transition zone between the hyperarid Saharan Desert and the Guinean and GuineoCongolian region characterized by wet subtropical climate (Fig. 7A). In marked contrast, positive $\Delta\varepsilon_{Hf\ CLAY}$ values are mostly encountered in the subtropical regions of the uppermost Upper Niger catchment and in the lower course of the Niger and Benue rivers (Fig. 7A). Despite the above-mentioned evidence for a strong 'zircon effect' on $\Delta\varepsilon_{Hf\ CLAY}$ variability at the catchment scale, this observation suggests that climate also plays a significant role in controlling the degree of Nd-Hf isotope decoupling in the studied clay fractions. Strikingly, a similar relationship can be inferred between $\Delta\varepsilon_{Hf\ CLAY}$ and annual dust deposition rates in West Africa (Fig. 7B), with higher $\Delta\varepsilon_{Hf\ CLAY}$ values occurring counter-intuitively in areas subject to higher dust deposition fluxes. These total deposition rates represent modelled estimates of the sum of both dry and wet dust deposition during the year (Schepanski, 2018). While dry deposition presumably accounts for preferential deposition of dense accessory minerals by gravitational settling during the Harmattan (winter) season (as discussed in Section 5.2 above), wet deposition associated with summer precipitation generally represents the dominant removal process for mineral aerosol in West Africa (Schepanski et al., 2009; Marticorena et al., 2017; Schepanski, 2018). The apparent relationship between $\Delta\varepsilon_{Hf\ CLAY}$ values and annual dust deposition is further confirmed when examining the variability of $\Delta\varepsilon_{Nd\ CLAY\text{-}SAND}$ across the Niger watershed (the degree of size-dependent Nd isotope decoupling in studied river sediment samples), because high $\Delta\varepsilon_{Nd\ CLAY\text{-}SAND}$ values in the studied samples, indirectly suggestive of high dust inputs, generally also coincide with both high $\Delta\varepsilon_{Hf\ CLAY}$ and annual dust deposition rates (Fig. 7D).

Taken together, these findings suggest that Saharan dust deposition plays an important role in controlling chemical weathering rates and associated phosphorus release in West Africa. In tropical regions, enhanced alteration of phosphate-bearing accessory minerals such as

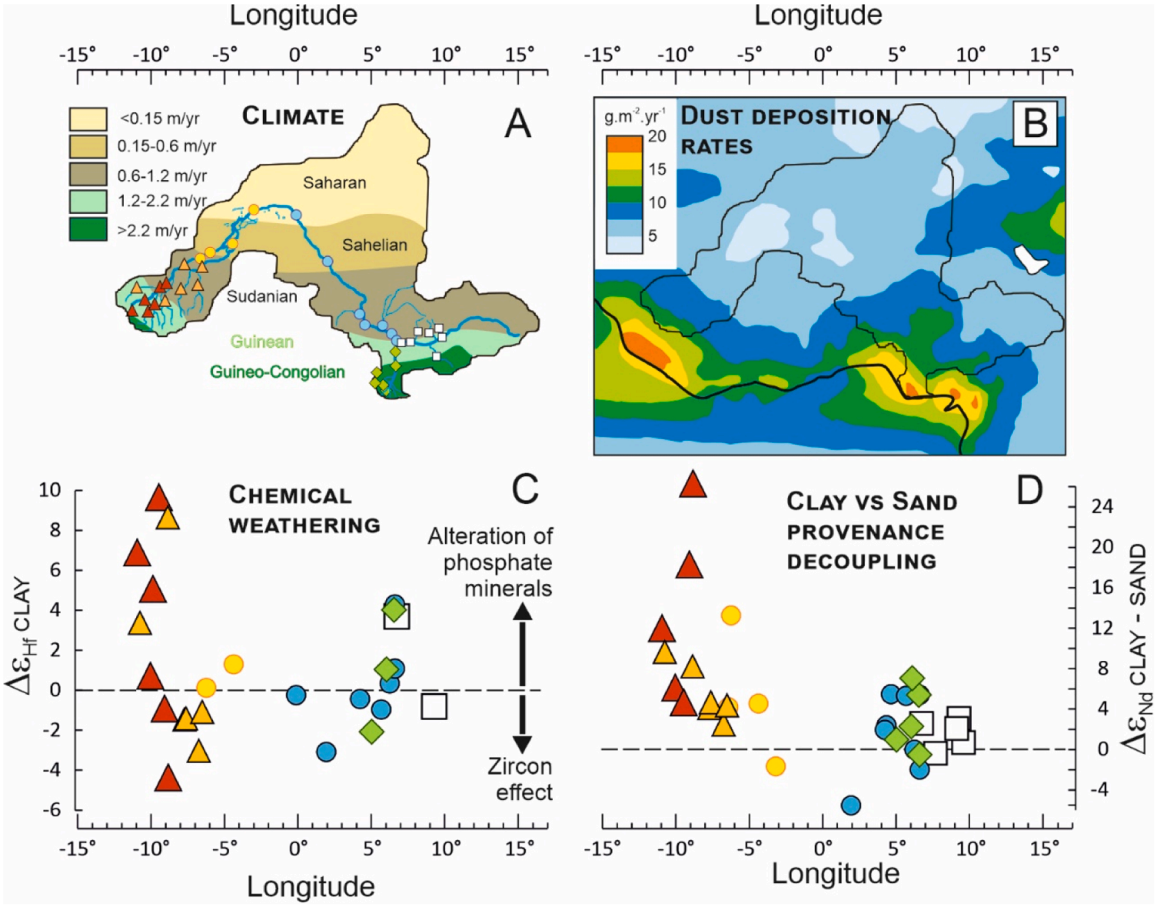

Fig. 7. Relationships among climate, dust deposition and chemical weathering of phosphate-bearing minerals in West Africa. (A) The five climate regions of the Niger River Basin (CILSS, 2016). (B) Annual total dust deposition fluxes (g/m^2) averaged over the 10-year period 2003–2012 (Schepanski, 2018). (C) Longitudinal evolution of the degree of Nd-Hf isotope decoupling ($\Delta\varepsilon_{Hf\ CLAY}$) across the Niger River Basin. $\Delta\varepsilon_{Hf\ CLAY}$ corresponds to the vertical deviation of Hf isotopes relative to the Clay Array in the ε_{Nd} vs ε_{Hf} diagram; positive $\Delta\varepsilon_{Hf\ CLAY}$ values are interpreted as reflecting enhanced alteration of radiogenic phosphate minerals in soils (Bayon et al., 2016). (D) ε_{Nd} differences between clay and corresponding sand fractions of Niger River sediments ($\Delta\varepsilon_{Nd\ CLAY\text{-}SAND}$), indicating the degree of provenance decoupling in clay-sand pairs.

apatite and monazite is known to release substantial amounts of light-REE and P in surface environments, which typically results in the formation of discrete crystals of secondary phosphate LREE-minerals in close association with kaolinite aggregates (Banfield and Eggleton, 1989). Secondary phosphate mineral phases such as LREE-rich APS minerals of the crandallite series (e.g., florencite) and rhabdophane are ubiquitous in tropical soils and laterites and can dominate the light-REE budget in kaolinite aggregates (Braun et al., 1990; Berger et al., 2008, 2014). In tropical soils, the formation of Th-rich rhabdophane commonly relates to the alteration of monazite (Berger et al., 2008). On this basis, and in full agreement with our SEM-EDS observations (Fig. 4B), we propose that the occurrence of high $\Delta\varepsilon_{Hf\ CLAY}$ values across the Niger River basin directly relates to the formation of secondary phosphate minerals in subtropical soils, as recently inferred from an investigation of marine clays collected near the mouth of the Congo River (Bayon et al., 2023). Importantly, the evidence that high $\Delta\varepsilon_{Hf\ CLAY}$ values in this study also coincide with pronounced Nd isotope decoupling in clay-sand pairs further indicates that P and light-REE in corresponding subtropical soils of the Niger catchment mostly derive from chemical weathering of dust-borne phosphate-bearing minerals (e.g., monazite). This hypothesis is fully consistent with findings inferred from a previous investigation of lateritic soils in southern Cameroon (Viers and Wasserburg, 2004), in which a pronounced Nd isotope decoupling between the bedrock and overlying soils (up to ~18 ε-units) was attributed to high mobility of light-REE and P, following preferential alteration of atmospheric inputs. On this basis, we argue that the combination of high precipitation levels and enhanced Saharan dust deposition in subtropical West Africa promotes the alteration of wind-blown accessory phosphate minerals in surface environments.

5.4. *Significance of atmospheric inputs to erosional and chemical weathering fluxes in subtropical catchments*

Our results provide direct evidence that Saharan dust deposition represents a first-order factor controlling sediment yield in the Niger River basin. Estimates for annual dust deposition in West Africa vary largely in the literature from a few to hundreds of grams per m^2 (e.g., Kalu, 1979; Schepanski, 2018; Marticorena et al., 2017). Continuous field monitoring at different stations over the past decade indicates annual deposited mass fluxes ranging from 75 to 183 g/m^2 in West Africa, with an estimated average of about 100 g/m^2 per year (Marticorena et al., 2017). As mentioned above, a significant proportion (~90 %) of the sediment carried by the Niger River to the Gulf of Guinea is contributed by the Benue River (Pastore et al., 2023). Using 100 g/m^2 for annual dust deposition and assuming quantitative dust transfer from the Benue catchment (~319 × 10^3 km^2) to the suspended load of the Lower Niger, we estimate that about 32 Mt of Saharan dust could be delivered annually to the Atlantic Ocean via the Niger River. Such back-of-the-envelope calculation would indicate that wind-blown dust might account for even up to 80 % of the annual suspended discharge of the Niger River (~40 Mt; Milliman and Farnsworth, 2013), an estimate that – considering its inherent large uncertainty – is not entirely

inconsistent with the estimated 40 ± 20 % contribution inferred from Nd isotope data. By analogy, this finding implies that large river systems from other regions subject to high dust deposition worldwide (e.g., South Asia, Eastern Asia) could equally export substantial amounts of aeolian dust, suggesting possible bias for calculated physical denudation rates at the catchment scale.

A further major implication of our results is that preferential alteration of Saharan dust acts as a major source of phosphorus and other nutrients to surface environments in West Africa, as long proposed for far distal regions of the Amazon Basin and Caribbean Islands (Swap et al., 1992; Okin et al., 2004; Koren et al., 2006; Pett-Ridge, 2009; Bristow et al., 2010). In low-elevation shield areas characterized by thick soil profiles and transport-limited weathering conditions, chemical weathering fluxes generally scale positively with the rate of supply of available particulate material (West, 2012). In this context, our results imply that, in transport-limited subtropical environments adjacent to large desert areas, enhanced delivery of mineral dust to surface sediments directly translates into higher chemical weathering fluxes. While further investigations would be required to directly quantify the impact of Saharan dust dissolution on dissolved riverine fluxes in the Niger River basin, this finding is consistent with published data for Nd isotopes in river waters from southern Cameroon, which display ε_{Nd} signatures similar to surrounding lateritic soils that are strongly affected by preferential dissolution of dust inputs (Viers and Wasserburg, 2004). Finally, our interpretation echoes previous assumptions that sustained delivery of airborne particles to subtropical regions located along major dust trajectories could account for extensive laterite formation worldwide (Brimhall et al., 1988).

6. Conclusions

Our geochemical investigation of clay from the Niger River basin provides direct evidence that Saharan dust profoundly influences sediment yield and continental weathering in West Africa. Substantial amounts of Harmattan dust blown from the Bodélé Depression to surface sediments in West Africa are remobilized across the Niger River basin, contributing to ~40 % of the fine sediment discharge exported to the Atlantic Ocean. In the Niger catchment, the degree of alteration of phosphate-bearing minerals directly relates to wet dust deposition and preferential dissolution of wind-blown particles, suggesting that Saharan dust plays an important role in controlling chemical weathering fluxes and phosphorus release in subtropical West Africa. These findings reinforce the hypothesis that large deserts act as a major source of nutrients to adjacent continental areas located along dust plume trajectories.

CRediT authorship contribution statement

Germain Bayon: Writing – original draft, Project administration, Methodology, Investigation, Funding acquisition, Formal analysis, Conceptualization. **Eduardo Garzanti:** Writing – review & editing, Resources. **Pedro Dinis:** Writing – review & editing, Formal analysis. **Daniel Beaufort:** Writing – review & editing, Formal analysis. **Jean-Alix Barrat:** Writing – review & editing, Investigation. **Yoan Germain:** Writing – review & editing, Formal analysis. **Anne Trinquier:** Writing – review & editing, Formal analysis. **Marta Barbarano:** Writing – review & editing, Resources. **Brume Overare:** Writing – review & editing, Resources. **Olusegun Adeaga:** Writing – review & editing, Resources. **Nadine Braquet:** Writing – review & editing, Resources.

Declaration of competing interest

The authors declare that they have no known competing financial interests or personal relationships that could have appeared to influence the work reported in this paper.

Data availability

All data associated with this study are reported in Table 1 and Supplementary Table S1.

Acknowledgments

We are most grateful to Boubacar Baïlo Diakité and Diarra Diallo of the National Hydraulic Directorate of Conakry (DNH-Guinea) and to Boubacar Sidibé and Adama Mariko of the National Hydraulic Directorate of Bamako (DNH-Mali) for conducting sediment sampling in Guinea and Mali under the supervision of IRD-Bamako. We also greatly acknowledge Ibrahim Mamadou (University of Zinder, Niger) for providing samples from Niger and students and collaborators at the Federal University of Petroleum Resources Effurun (Ilo David Adeyemi, Ogefere Onoharigho, Igbinosa Osaze Temple, Solomon Awakessien, Efenudu Benjamin) and Nasarawa State University (Christabel Otite) for providing samples from Nigeria. M. Rovere (IFREMER) is warmly thanked for the preparation of slides. Analytical work for geochemical analyses was funded by a grant to G.B. from the French National Research Agency (ANR-20-CE01–0003). We gratefully acknowledge Andrew Jacobson for editorial handling and two anonymous reviewers for providing insightful comments.

Supplementary materials

Supplementary material associated with this article can be found, in the online version, at doi:10.1016/j.epsl.2024.118845.

References

Aarons, S.M., Aciego, S.M., Gleason, J.D., 2013. Variable Hf-Sr-Nd radiogenic isotopic compositions in a Saharan dust storm over the Atlantic: implications for dust flux to oceans, ice sheets and the terrestrial biosphere. Chem. Geol. 349-350, 18–26.

Abouchami, W., Näthe, K., Kumar, A., Galer, S.J., Jochum, K.P., Williams, E., Horbe, A. M., Rosa, J.W., Balsam, W., Adams, D., Mezger, K., 2013. Geochemical and isotopic characterization of the Bodélé Depression dust source and implications for transatlantic dust transport to the Amazon Basin. Earth Planet. Sci. Lett. 380, 112–123.

Afeti, G.M., Resch, F.J., 2000. Physical characteristics of Saharan dust near the Gulf of Guinea. Atmos. Environ. 34, 1273–1279.

Albarède, F., Simonetti, A., Vervoort, J.D., Blichert-Toft, J., Abouchami, W., 1998. A Hf-Nd isotopic correlation in ferromanganese nodules. Geophys. Res. Lett. 25, 3895–3898.

Armitage, S.J., Bristow, C.S., Drake, N.A., 2015. West African monsoon dynamics inferred from abrupt fluctuations of Lake Mega-Chad. Proc. Nat. Acad. Sci. 112, 8543–8548.

Banfield, J.F., Eggleton, R.A., 1989. Apatite replacement and rare earth mobilization, fractionation, and fixation during weathering. Clay Clay Miner 37, 113–127.

Barkley, A.E., Prospero, J.M., Mahowald, N., Hamilton, D.S., Popendorf, K.J., Oehlert, A. M., Pourmand, A., Gatineau, A., Panechou-Pulcherie, K., Blackwelder, P., Gaston, C. J., 2019. African biomass burning is a substantial source of phosphorus deposition to the Amazon, Tropical Atlantic Ocean, and Southern Ocean. Proc. Nat. Acad. Sci. 116, 16216–16221.

Barkley, A.E., Pourmand, A., Longman, J., Sharifi, A., Prospero, J.M., Panechou, K., Bakker, N., Drake, N., Guinoiseau, D., Gaston, C.J., 2022. Interannual variability in the source location of north African dust transported to the Amazon. Geophys. Res. Lett. 49 e2021GL097344.

Barrat, J.A., Keller, F., Amossé, J., Taylor, R.N., Nesbitt, R.W., Hirata, T., 1996. Determination of rare earth elements in sixteen silicate reference samples by ICP-MS after Tm addition and ion exchange separation. Geostand. Newslett. 20, 133–139.

Bationo, A., Mokwunye, A.U., 1991. Alleviating soil fertility constraints to increased crop production in West Africa: the experience in the Sahel. Exp. Sahel. Fertil. Res. 29, 95–115. https://doi.org/10.1007/BF01048992, 195-215.

Bayon, G., Vigier, N., Burton, K.W., Jean Carignan, A.B., Etoubleau, J., Chu, N.C., 2006. The control of weathering processes on riverine and seawater hafnium isotope ratios. Geology 34, 433–436.

Bayon, G., Burton, K.W., Soulet, G., Vigier, N., Dennielou, B., Etoubleau, J., Ponzevera, E., German, C.R., Nesbitt, R.W., 2009. Hf and Nd isotopes in marine sediments: constraints on global silicate weathering. Earth Planet. Sci. Lett. 277, 318–326.

Bayon, G., Toucanne, S., Skonieczny, C., André, L., Bermell, S., Cheron, S., Dennielou, B., Etoubleau, J., Freslon, N., Gauchery, T., Germain, Y., Jorry, S.J., Ménot, G., Monin, L., Ponzevera, E., Rouget, M.L., Tachikawa, K., Barrat, J.A., 2015. Rare Earth

elements and neodymium isotopes in World river sediments revisited. Geochim. Cosmochim. Acta 170, 17–38.
Bayon, G., Skonieczny, C., Delvigne, C., Toucanne, S., Bermell, S., Ponzevera, E., André, L., 2016. Environmental Hf–Nd isotopic decoupling in World river clays. Earth Planet. Sci. Lett. 438, 25–36.
Bayon, G., Bindeman, I.N., Trinquier, A., Retallack, G.J., Bekker, A., 2022. Long-term evolution of terrestrial weathering and its link to Earth's oxygenation. Earth Planet. Sci. Lett. 584, 117490.
Bayon, G., Giresse, P., Chen, H., Rouget, M.L., Gueguen, B., Moizinho, G.R., Barrat, J.A., Beaufort, D., 2023. The Behavior of Rare Earth Elements during Green Clay Authigenesis on the Congo Continental Shelf. Minerals 13, 1081. https://doi.org/10.3390/min13081081.
Berger, A., Gnos, E., Janots, E., Fernandez, A., Giese, J., 2008. Formation and composition of rhabdophane, bastnäsite and hydrated thorium minerals during alteration: implications for geochronology and low-temperature processes. Chem. Geol. 254, 238–248.
Berger, A., Janots, E., Gnos, E., Frei, R., Bernier, F., 2014. Rare earth element mineralogy and geochemistry in a laterite profile from Madagascar. Appl. Geochem. 41, 218–228.
Boher, M., Abouchami, W., Michard, A., Albarede, F., Arndt, N.T., 1992. Crustal growth in West Africa at 2.1 Ga. J. Geophys. Res. Solid Earth 97, 345–369.
Bouvier, A., Vervoort, J.D., Patchett, P.J., 2008. The Lu–Hf and Sm–Nd isotopic composition of CHUR: constraints from unequilibrated chondrites and implications for the bulk composition of terrestrial planets. Earth Planet. Sci. Lett. 273, 48–57.
Bozlaker, A., Prospero, J.M., Price, J., Chellam, S., 2018. Linking Barbados mineral dust aerosols to North African sources using elemental composition and radiogenic Sr, Nd, and Pb isotope signatures. J. Geophys. Res. Atmos. 123, 1384–1400.
Braun, J.J., Pagel, M., Muller, J.P., Bilong, P., Michard, A., Guillet, B., 1990. Cerium anomalies in lateritic profiles. Geochim. Cosmochim. Acta 54, 781–795.
Brimhall, G.H., Lewis, C.J., Ague, J.J., Dietrich, W.E., Hampel, J., Teague, T., Rix, P., 1988. Metal enrichment in bauxites by deposition of chemically mature aeolian dust. Nature 333, 819–824.
Bristow, C.S., Hudson-Edwards, K.A., Chappell, A., 2010. Fertilizing the Amazon and equatorial Atlantic with West African dust. Geophys. Res. Lett. 37, L14807.
Chen, H., Bayon, G., Xu, Z., Li, T., 2023. Hafnium isotope evidence for enhanced weatherability at high southern latitudes during Oceanic Anoxic Event 2. Earth Planet. Sci. Lett. 601, 117910.
CILSS, 2016. Landscapes of West Africa – A Window On a Changing World. U.S. Geological Survey, EROS, 47914 252nd St, Garretson, SD 57030, U.S.A.
Dausmann, V., Gutjahr, M., Frank, M., Kouzmanov, K., Schaltegger, U., 2019. Experimental evidence for mineral-controlled release of radiogenic Nd, Hf and Pb isotopes from granitic rocks during progressive chemical weathering. Chem. Geol. 507, 64–84.
Deynoux, M., Affaton, P., Trompette, R., Villeneuve, M., 2006. Pan-African tectonic evolution and glacial events registered in Neoproterozoic to Cambrian cratonic and foreland basins of West Africa. J. Afr. Earth Sci. 46, 397–426.
Falaiye, O.A., Aweda, F.O., 2018. Trace metals and mineral composition of harmattan dust haze in Ilorin city, Kwara state, Nigeria. J. Appl. SCI Environ. Manag. 22, 281–285.
Garçon, M., Chauvel, C., France-Lanord, C., Huyghe, P., Lavé, J., 2013. Continental sedimentary processes decouple Nd and Hf isotopes. Geochim. Cosmochim. Acta. 121, 177–195.
Goudie, A.S., Middleton, N.J., 2001. Saharan dust storms: nature and consequences. Earth Sci. Rev. 56, 179–204.
Grousset, F.E., Parra, M., Bory, A., Martinez, P., Bertrand, P., Shimmield, G., Ellam, R.M., 1998. Saharan wind regimes traced by the Sr–Nd isotopic composition of subtropical Atlantic sediments: last glacial maximum vs today. Quat. Sci. Rev. 17, 395–409.
Guinoiseau, D., Singh, S.P., Galer, S.J.G., Abouchami, W., Bhattacharyya, R., Kandler, K., Bristow, C., Andreae, M.O., 2022. Characterization of Saharan and Sahelian dust sources based on geochemical and radiogenic isotope signatures. Quat. Sci. Rev. 293, 107729.
Jewell, A.M., Drake, N., Crocker, A.J., Bakker, N.L., Kunkelova, T., Bristow, C.S., Cooper, M.J., Milton, J.A., Wilson, P.A., 2021. Three North African dust source areas and their geochemical fingerprint. Earth Planet. Sci. Lett. 554, 116645.
Jickells, T.D., An, Z.S., Andersen, K.K., Baker, A.R., Bergametti, G., Brooks, N., Duce, R. A., Hunter, K.A., Kawahata, H., Kubilay, N., laRoche, J., Liss, P.S., Mahowald, N., Prospero, J.L., Ridgwell, A.J., Tegen, I., Torres, R., 2005. Global iron connections between desert dust, ocean biogeochemistry, and climate. Science 308, 67–71.
Kalu, A.E., 1979. The African dust plume: its characteristics and propagation across West Africa in winter. In: Morales, C. (Ed.), Saharan Dust: Mobilization, Transport, Deposition. Wiley, New york, pp. 95–118 (1979).
Koren, I., Kaufman, Y.J., Washington, R., Todd, M.C., Rudich, Y., Martins, J.V., Rosenfeld, D., 2006. The Bodélé depression: a single spot in the Sahara that provides most of the mineral dust to the Amazon forest. Environ. Res. Lett. 1, 014005.
Kouamelan, A.N., Delor, C., Peucat, J.J., 1997. Geochronological evidence for reworking of Archean terrains during the early Proterozoic (2.1 Ga) in the western Cote d'Ivoire (Man Rise-West African Craton). Precambrian Res 86, 177–199.
Laurent, B., Marticorena, B., Bergametti, G., Léon, J.F., Mahowald, N.M., 2008. Modeling mineral dust emissions from the Sahara desert using new surface properties and soil database. J. Geophys. Res. Atmos. 113 https://doi.org/10.1029/2007JD009484. D14218.
Lebrun, E., Thébaud, N., Miller, J., Ulrich, S., Bourget, J., Terblanche, O., 2016. Geochronology and lithostratigraphy of the Siguiri district: implications for gold mineralisation in the Siguiri Basin (Guinea, West Africa). Precambrian Res 274, 136–160.
Mahé, G., Bamba, F., Soumaguel, A., Orange, D., Olivry, J.C., 2009. Water losses in the inner delta of the River Niger: water balance and flooded area. Hydrol. Process. 23, 3157–3160.
Marticorena, B., Chatenet, B., Rajot, J.L., Bergametti, G., Deroubaix, A., Vincent, J., Kouoi, A., Schmechtig, C., Coulibaly, M., Diallo, A., Koné, I., 2017. Mineral dust over west and central Sahel: seasonal patterns of dry and wet deposition fluxes from a pluriannual sampling (2006–2012). J. Geophys. Res. Atmos. 122, 1338–1364.
McTainsh, G.H., Walker, P.H., 1982. Nature and distribution of Harmattan dust. Z. Geomorphol. 26, 417–435.
Meyer, I., Davies, G.R., Stuut, J.B.W., 2011. Grain size control on Sr-Nd isotope provenance studies and impact on paleoclimate reconstructions: an example from deep-sea sediments offshore NW Africa. Geochem. Geophys. Geosyst. 12.
Milliman, J.D., Farnsworth, K.L., 2013. River discharge to the coastal ocean: a global synthesis. Cambridge University Press.
Ofoegbu, C.O., 1985. A review of the geology of the Benue Trough. Nigeria. J. Afr. Earth Sci. 3, 283–291.
Öhlander, B., Ingri, J., Land, M., Schöberg, H., 2000. Change of Sm-Nd isotope composition during weathering of till. Geochim. Cosmochim. Acta 64, 813–820.
Okin, G.S., Mahowald, N., Chadwick, O.A., Artaxo, P., 2004. Impact of desert dust on the biogeochemistry of phosphorus in terrestrial ecosystems. Glob. Biogeochem. Cycl. 18 https://doi.org/10.1029/2003GB002145. GB2005.
Parra-Avila, L.A., Belousova, E., Fiorentini, M.L., Baratoux, L., Davis, J., Miller, J., McCuaig, T.C., 2016. Crustal evolution of the Paleoproterozoic Birimian terranes of the Baoulé-Mossi domain, southern West African Craton: u–Pb and Hf-isotope studies of detrital zircons. Precambrian Res 274, 25–60.
Pastore, G., Garzanti, E., Vermeesch, P., Bayon, G., Resentini, A., Braquet, N., Overare, B., 2023. The zircon story of the niger river: time-structure maps of the west african craton and discontinuous propagation of provenance signals across a disconnected sediment-routing system. J. Geophys. Res. Earth Surf. 128 e2023JF007342.
Patchett, P.J., White, W.M., Feldmann, H., Kielinczuk, S., Hofmann, A.W., 1984. Hafnium/rare earth element fractionation in the sedimentary system and crustal recycling into the Earth's mantle. Earth Planet. Sci. Lett. 69, 365–378.
Pett-Ridge, J.C., 2009. Contributions of dust to phosphorus cycling in tropical forests of the Luquillo Mountains. Puerto Rico. Biogeochem. 94, 63–80.
Pourmand, A., Prospero, J.M., Sharifi, A., 2014. Geochemical fingerprinting of trans-Atlantic African dust based on radiogenic Sr-Nd-Hf isotopes and rare earth element anomalies. Geology 42, 675–678.
Prospero, J.M., Ginoux, P., Torres, O., Nicholson, S.E., Gill, T.E., 2002. Environmental characterization of global sources of atmospheric soil dust identified with the Nimbus 7 Total Ozone Mapping Spectrometer (TOMS) absorbing aerosol product. Rev. Geophys. 40, 2. -1.
Rickli, J., Frank, M., Baker, A.R., Aciego, S., De Souza, G., Georg, R.B., Halliday, A.N., 2010. Hafnium and neodymium isotopes in surface waters of the eastern Atlantic Ocean: implications for sources and inputs of trace metals to the ocean. Geochim. Cosmochim. Acta 74, 540–557.
Schepanski, K., Tegen, I., Macke, A., 2009. Saharan dust transport and deposition towards the tropical northern Atlantic. Atmos. Chem. Phys. 9, 1173–1189.
Schepanski, K., 2018. Transport of mineral dust and its impact on climate. Geosciences 8, 151.
Swap, R., Garstang, M., Greco, S., Talbot, R., Kållberg, P., 1992. Saharan dust in the Amazon Basin. Tellus B 44, 133–149.
Thiéblemont, D., Goujou, J.C., Egal, E., Cocherie, A., Delor, C., Lafon, J.M., Fanning, C. M., 2004. Archean evolution of the Leo Rise and its Eburnean reworking. J. Afr. Earth Sci. 39, 97–104.
Utah, E.U., Tsor, J.O., Makama, E.K., 2005. The harmattan haze in three Nigerian cities: concentration, size and settling velocity. Niger. J. Phys. 17, 92–98.
van der Does, M., Pourmand, A., Sharifi, A., Stuut, J.B.W., 2018. North African mineral dust across the tropical Atlantic Ocean: insights from dust particle size, radiogenic Sr-Nd-Hf isotopes and rare earth elements (REE). Aeolian Res 33, 106–116.
Vervoort, J.D., Patchett, P.J., Blichert-Toft, J., Albarède, F., 1999. Relationships between Lu–Hf and Sm–Nd isotopic systems in the global sedimentary system. Earth Planet. Sci. Lett. 168, 79–99.
Vervoort, J.D., Plank, T., Prytulak, J., 2011. The Hf–Nd isotopic composition of marine sediments. Geochim. Cosmochim. Acta 75, 5903–5926.
Viers, J., Wasserburg, G.J., 2004. Behavior of Sm and Nd in a lateritic soil profile. Geochim. Cosmochim. Acta 68, 2043–2054.
West, A.J., 2012. Thickness of the chemical weathering zone and implications for erosional and climatic drivers of weathering and for carbon-cycle feedbacks. Geology 40, 811–814.
Wilke, B.M., Duke, B.J., Jimoh, W.L.O., 1984. Mineralogy and chemistry of Harmattan dust in northern Nigeria. Catena 11, 91–96.
Yu, Y., Kalashnikova, O.V., Garay, M.J., Lee, H., Notaro, M., Campbell, J.R., Marquis, J., Ginoux, P., Okin, G.S., 2020. Disproving the bodélé depression as the primary source of dust fertilizing the Amazon Rainforest. Geophys. Res. Lett. 47 e2020GL088020.
Zhao, W., Sun, Y., Balsam, W., Lu, H., Liu, L., Chen, J., Ji, J., 2014. Hf-Nd isotopic variability in mineral dust from Chinese and Mongolian deserts: implications for sources and dispersal. Sci. Rep. 4, 5837. https://doi.org/10.1038/srep05837.
Zhao, W., Balsam, W., Williams, E., Long, X., Ji, J., 2018. Sr–Nd–Hf isotopic fingerprinting of transatlantic dust derived from North Africa. Earth Planet. Sci. Lett. 486, 23–31.